◆ Human Brain Mapping 36:199–212 (2015) ◆

Cognitive Impairment and Resting-State Network Connectivity in Parkinson's Disease

Hugo-Cesar Baggio,[1] Bàrbara Segura,[1] Roser Sala-Llonch,[1] Maria-José Marti,[2,3] Francesc Valldeoriola,[2,3] Yaroslau Compta,[2,3] Eduardo Tolosa,[2,3,4] and Carme Junqué[1,3,4]*

[1]*Departament de Psiquiatria i Psicobiologia Clínica, Universitat de Barcelona, Barcelona, Catalonia, Spain*
[2]*Parkinson's Disease and Movement Disorders Unit, Neurology Service, Institut Clínic de Neurociències (ICN), Hospital Clínic de Barcelona, Barcelona, Catalonia, Spain*
[3]*Centro de Investigación Biomédica en Red sobre Enfermedades Neurodegenerativas (CIBERNED), Hospital Clínic de Barcelona, Barcelona, Catalonia, Spain*
[4]*Institut d'Investigacions Biomèdiques August Pi i Sunyer (IDIBAPS), Barcelona, Catalonia, Spain*

Abstract: The purpose of this work was to evaluate changes in the connectivity patterns of a set of cognitively relevant, dynamically interrelated brain networks in association with cognitive deficits in Parkinson's disease (PD) using resting-state functional MRI. Sixty-five nondemented PD patients and 36 matched healthy controls were included. Thirty-four percent of PD patients were classified as having mild cognitive impairment (MCI) based on performance in attention/executive, visuospatial/visuoperceptual (VS/VP) and memory functions. A data-driven approach using independent component analysis (ICA) was used to identify the default-mode network (DMN), the dorsal attention network (DAN) and the bilateral frontoparietal networks (FPN), which were compared between groups using a dual-regression approach controlling for gray matter atrophy. Additional seed-based analyses using a priori defined regions of interest were used to characterize local changes in intranetwork and internetwork connectivity. Structural group comparisons through voxel-based morphometry and cortical thickness were additionally performed to assess associated gray matter atrophy. ICA results revealed reduced connectivity between the DAN and right frontoinsular regions in MCI patients, associated with worse performance in attention/executive functions. The DMN displayed increased connectivity with medial and lateral occipito-parietal regions in MCI patients, associated with worse VS/VP performance, and with occipital reductions in cortical thickness. In line with data-driven results, seed-based analyses mainly revealed reduced within-DAN, within-DMN and DAN-FPN connectivity, as well as loss of normal DAN-DMN anticorrelation in MCI patients. Our findings demonstrate differential connectivity changes affecting the networks evaluated, which we hypothesize to be

Additional Supporting Information may be found in the online version of this article.

Contract grant sponsor: Spanish Ministry of Science and Innovation; Contract grant number: PSI2013- 41393 (to C.J.; H.C.B.; and B.S.); Contract grant sponsor: Generalitat de Catalunya; Contract grant number: 2014SGR98 (to C.J.) and 2011FI_B 00045 (to H.C.B.), Contract grant sponsor: CIBERNED

*Correspondence to: Prof. Carme Junqué, Department of Psychiatry and Clinical Psychobiology. University of Barcelona, Casanova 143 (08036) Barcelona, Spain. E-mail: cjunque@ub.edu

Received for publication 2 May 2014; Revised 29 July 2014; Accepted 20 August 2014.

DOI: 10.1002/hbm.22622
Published online 28 August 2014 in Wiley Online Library (wileyonlinelibrary.com).

related to the pathophysiological bases of different types of cognitive impairment in PD. *Hum Brain Mapp 36:199–212, 2015.*

Key words: Parkinson's disease; mild cognitive impairment; fMRI; resting-state connectivity

INTRODUCTION

In the framework of an integrated model of brain function, neuroimaging studies have demonstrated the relevance of a set of dynamically interrelated brain intrinsic connectivity networks (ICNs) considered to play an important role in cognitive processing: the default-mode network (DMN), the dorsal attention network (DAN), and the frontoparietal networks (FPN) [Sala-Llonch et al., 2012; Seeley et al., 2007; Spreng et al., 2010]. These networks can be evaluated through resting-state functional techniques, and their role as part of the functional substrates of cognitive manifestations of neuropathological processes can be assessed [Smith et al., 2009; Spreng et al., 2010].

Cognitive impairment is an important cause of disability in Parkinson's disease (PD), and patients with mild cognitive impairment (MCI) are at a higher risk of subsequently developing dementia [Williams-Gray et al., 2007], which over time affects around 75% of patients (see [Aarsland and Kurz, 2010]). In a previous study with the same subject sample, we used a graph-theoretical approach to assess changes in global patterns of resting-state functional connectivity and found that MCI in PD was associated with widespread connectivity decrements as well as some increments [Baggio et al., 2014]. Since previous studies in PD have mainly focused on changes affecting the DMN [Eimeren and Monchi, 2009; Krajcovicova et al., 2012; Rektorova et al., 2012; Tessitore et al., 2012], little is known about how the disease affects other resting-state ICNs.

Our goal in this study was to evaluate connectivity changes in a set of brain networks—the DMN, the DAN, and the bilateral FPN [Spreng et al., 2013]. Specifically, our objective was, in a first step, to assess changes in overall ICN connectivity in the presence of MCI in a large sample of nondemented PD patients through a data-driven independent component analysis (ICA) resting-state functional MRI approach. We also aimed to assess the relationship between changes in patterns of network connectivity and performance in the cognitive functions most frequently affected in PD without dementia, that is, attention/executive (A/E), episodic memory, and visuospatial/visuoperceptual (VS/VP) [Aarsland et al., 2009; Elgh et al., 2009; Muslimovic et al., 2005]. In a second step, we aimed to evaluate the local patterns of ICN functional connectivity disruption associated with the presence of MCI in PD using an a priori seed-based analysis. Additionally, we have performed structural analyses to assess whether connectivity changes were accompanied by gray matter (GM) atrophy.

MATERIALS AND METHODS

Participants

Eighty-four nondemented PD patients and 38 healthy controls (HC) matched for age, sex, and years of education were recruited [Baggio et al., 2014]. The inclusion criterion for patients was the fulfillment of UK PD Society Brain Bank diagnostic criteria for PD. Exclusion criteria were: (i) MMSE $\leq$25 or dementia [Emre et al., 2007], (ii) Hoehn and Yahr (HY) score $>$ III, (iii) significant psychiatric, neurological or systemic comorbidity, (iv) significant pathological MRI findings other than mild white-matter (WM) hyperintensities in the FLAIR sequence, and (v) root-mean-square head motion $>$ 0.3 mm translation or 0.6° rotation. Four patients were excluded due to macroscopic movement, 14 due to head motion $>$ 0.3 mm translation or $>$ 0.6° rotation, and one for being an outlier in dual-regression analyses. Two HC were excluded due to microvascular WM changes, leaving a final sample of 65 PD patients and 36 HC. All patients except one were taking antiparkinsonian medication; all assessments were done in the *on* state. Levodopa equivalent daily dose (LEDD) was calculated as suggested by Tomlinson et al. [Tomlinson et al., 2010]. Motor disease severity was evaluated using HY staging and the Unified Parkinson's Disease Rating Scale motor section (UPDRS-III). The study was approved by the ethics committee of the University of Barcelona. All subjects provided written informed consent to participate.

Neuropsychological Assessment

Attention/executive (backward minus forward digit spans; Trail-Making Test part A minus part B scores; phonemic fluency scores (words beginning with "*P*" produced in 60 s), and Stroop Color-Word Test interference scores), VS/VP (Benton's Visual Form Discrimination and Judgment of Line Orientation tests) and memory (Rey's Auditory Verbal Learning Test total learning and 20-min free recall scores) functions were tested in all subjects. *Z*-scores for each test and subject were calculated based on the HC group's means and standard deviations. Expected *z*-scores adjusted for age, sex, and education for each test and subject were calculated based on a multiple regression analysis performed in the HC group [Aarsland et al., 2009]. Subjects were classified as having MCI if the actual *z*-score for a test was $\geq$ 1.5 lower than the expected score in at least two tests in one domain or in one test per domain in at least two domains. As expected [Muslimovic et al., 2005], most MCI subjects had

deficits in more than one function, precluding the creation of patient groups with single-domain impairments. Composite *z*-scores for each domain were calculated by averaging the age, sex, and education-corrected *z*-scores of all tests within that domain.

MRI Acquisition

Structural T1-weighted images, functional resting-state images and FLAIR images were acquired on a 3T Siemens MRI scanner as previously described [Baggio et al., 2014].

Processing of fMRI

The preprocessing of resting-state images was performed with FSL release 5.0.5 (http://www.fmrib.ox.ac.uk/fsl/) and AFNI (http://afni.nimh.nih.gov/afni). Briefly, it included removal of the first five volumes to allow for T1 saturation effects, skull stripping, grandmean scaling and temporal filtering (bandpass filtering of 0.01–0.1 Hz).

To control for the effect of subject head movement, physiological artifacts (e.g., breathing and vascular) and other non-neural sources of signal variation on the estimation of connectivity, motion correction (using FSL's MCFLIRT), and regression of nuisance signals (six motion parameters, cerebrospinal fluid signal and WM signal) were performed. Cerebrospinal fluid and WM mean signals were determined by averaging the native-space functional time series of all voxels contained inside the corresponding masks obtained from the segmentation of the T1-weighted images using FSL's FAST. To remove the effects of volumes corrupted by motion, a scrubbing procedure, similar to that suggested by [Power et al., 2012], was applied. Briefly, root-mean square intensity differences between (unpreprocessed) volumes m and $m-1$ (DVARS) were calculated, indicating how much the global intensity of a volume changed compared to the previous timepoint. Volumes with DVARS above the 75th percentile + 1.5 times the interquartile range were considered as outliers and added to the confound matrices alongside the nuisance factors described above, thus removing their effects from the analyses. Functional images were registered to their corresponding T1-weighted images and then registered to the MNI-152 template using linear transformations, and subsequently smoothed with a 6-mm full-width at half maximum Gaussian kernel.

Additionally, individual subject translatory and rotatory head movements were calculated according to the following formula:

$$\frac{1}{M-1}\sum_{i=2}^{M}\sqrt{|x_i-x_{i-1}|^2+|y_i-y_{i-1}|^2+|z_i-z_{i-1}|^2},$$

where x_i, y_i, and z_i are translations or rotations in the three axes at timepoint i, and M is the total number of timepoints (145) [Liu et al., 2008].

To detect and quantify global (periventricular + deep) WM hyperintensity load, we used an automated segmentation procedure [Ithapu et al., 2014] using the FLAIR and T1-weighted images. Results are given in normalized volumes taking brain volume into account.

Quality Control

Despite rigorous head-motion exclusion criteria, rotational head motion was significantly higher in non-MCI (PD-NMCI) patients than in HC ($P = 0.028$, post hoc Bonferroni test), with no significant differences between HC and PD-MCI patients or between patient subgroups. Head motion data were added as covariates of no interest in intergroup comparisons.

Data-Driven Connectivity Assessment: ICA and Dual Regression

Preprocessed images were analyzed with MELODIC using a temporal-concatenation spatial ICA approach [Beckmann and Smith, 2004]. In this step, temporally and spatially coherent patterns of signal variation were extracted from functional images with a predetermined dimensionality of 25. To identify the ICNs of interest, spatial cross-correlation was performed in a two-step procedure: (1) Between the 25 extracted components and 20 resting-state ICN templates published in [Smith et al., 2009], which describes the DMN, right FPN, and left FPN; (2) Between the 25 extracted components and the combined main nodes of the DAN (see below) described from [Spreng et al., 2013]. The correspondence between the components and the strongest correlations with the ICNs of interested was further confirmed by visual inspection based on the descriptions available from reference studies [Fox et al., 2006; Raichle, 2011; Smith et al., 2009; Spreng et al., 2013].

The selected components were subsequently fed into a dual-regression analysis [Filippini et al., 2009]. In this step, each group component is used as a mask to extract a subject and component-specific mean time course, describing the temporal dynamics of each ICN. The time courses are then used as voxelwise regressors in a linear model against the individual fMRI sets to obtain subject-specific spatial maps for each ICN. Voxelwise one-sample *t*-tests were used to establish each group's significant ICN maps through nonparametric, permutation testing (5,000 permutations). To perform intergroup connectivity analyses, subjects' regression maps for each ICN of interest were compared using a voxelwise general linear model also with permutation testing (5,000 permutations). A binary mask created from the sum of all groups' thresholded maps for all four networks was used as a search volume for intergroup analyses to assess intranetwork and internetwork connectivity differences. Individual subjects' GM volume maps (see below) were entered as voxelwise

TABLE I. Anatomical regions used as network nodes for seed-based connectivity analyses

	Left hemisphere/midline		Right hemisphere	
Region	Network	Abbreviation	Network	Abbreviation
Frontal eye fields	DAN	DA left FEF	DAN	DA right FEF
Inferior precentral sulcus	DAN	DA left iPCS	DAN	DA right iPCS
Middle temporal motion complex	DAN	DA left MT	DAN	DA right MT
Superior occipital gyrus	DAN	DA left SOG	DAN	DA right SOG
Superior parietal lobule	DAN	DA left SPL	DAN	DA right SPL
Anterior medial prefrontal cortex	DMN	DMN amPFC		
Dorsal medial prefrontal cortex	DMN	DMN dmPFC		
Posterior cingulate cortex	DMN	DMN pCC		
Precuneus	DMN	DMN PCu		
Ventral medial prefrontal cortex	DMN	DMN vmPFC		
Anterior temporal lobe	DMN	DMN left aTL	DMN	DMN right aTL
Hippocampal formation	DMN	DMN left HF	DMN	DMN right HF
Inferior frontal gyrus	DMN	DMN left IFG	DMN	DMN right IFG
Posterior inferior parietal lobule	DMN	DMN left pIPL	DMN	DMN right pIPL
Superior frontal gyrus	DMN	DMN left SFG	FPN	FP right SFG
Superior temporal sulcus	DMN	DMN left STS	DMN	DMN right STS
Temporal parietal junction	DMN	DMN left TPJ	DMN	DMN right TPJ
Dorsal anterior cingulate cortex	FPN	FP daCC		
Medial superior prefrontal cortex	FPN	FP msPFC		
Anterior inferior parietal lobule	FPN	FP left aIPL	FPN	FP right aIPL
Anterior insula	FPN	FP left aINS	FPN	FP right aINS
Dorsolateral prefrontal cortex	FPN	FP left dlPFC	FPN	FP right dlPFC
Middle frontal gyrus BA 6	FPN	FP left MFG BA6	FPN	FP right MFG BA6
Middle frontal gyrus BA 9	FPN	FP left MFG BA9	FPN	FP right MFG BA9
Rostrolateral prefrontal cortex	FPN	FP left rlPFC	FPN	FP right rlPFC

Resting-state networks to which each node belongs is indicated: DAN (dorsal attention network), DMN (default mode network) or FPN (frontoparietal network).

regressors in intergroup comparisons to control for the effect of structural atrophy on connectivity measures; results were similar to those using global GM volume obtained with voxel-based morphometry (VBM) and mean cortical thickness obtained with FreeSurfer (see below) as covariates of no interest. In accordance with previous studies [Agosta et al., 2012; Brier et al., 2012], false-discovery rate (FDR) correction was used for multiple comparisons correction in intergroup testing ($P < 0.05$); to further control the occurrence of false-positive intergroup results, a cluster-size threshold of 100 voxels was applied to intergroup analyses as in [Agosta et al., 2012].

To evaluate the relationship between connectivity changes and cognitive performance, mean regression coefficients extracted from the clusters of significant PD-MCI-versus-PD-NMCI differences were correlated with demographic/clinical variables (age, education, UPDRS, BDI, LEDD). Subsequently, they were correlated with each individual's cognitive function scores (A/E, memory, VS/VP) while controlling for the other two functions. LEDD significantly correlated with intergroup differences in DAN connectivity; results including this measure as a covariate of no interest were similar to those without controlling for it.

Seed-Based Functional Connectivity Analysis Using A Priori-Defined Regions of Interest

In total, 43 nodes (10 DAN, 18 DMN, and 15 bilateral FPN nodes; see Table I) were included using the MNI coordinates described in [Spreng et al., 2013] and 10-mm radius circular masks. Voxels shared by more than one mask were excluded. The time series of all voxels inside each region were averaged, and the connectivity between two nodes was estimated using Pearson's correlation between their mean time series.

Our previous work evaluating the same sample [Baggio et al., 2014] showed that interregional connectivity differences tended to be more pronounced between PD-MCI and HC, a tendency also observed in the mean internetwork and intranetwork connectivity results obtained with seed-based analysis (Supporting Information Figure 1). We used the Jonckheere–Terpstra (JT) test [Bewick et al., 2004], a nonparametric test for ordered differences in three or more samples ($HC \geq PD\text{-}NMCI \geq PD\text{-}MCI$ or $HC \leq PD\text{-}NMCI \leq PD\text{-}MCI$, with at least one inequality being strict), to assess intergroup differences in functional connectivity. This analysis was done in two steps: (1) between mean intranetwork and

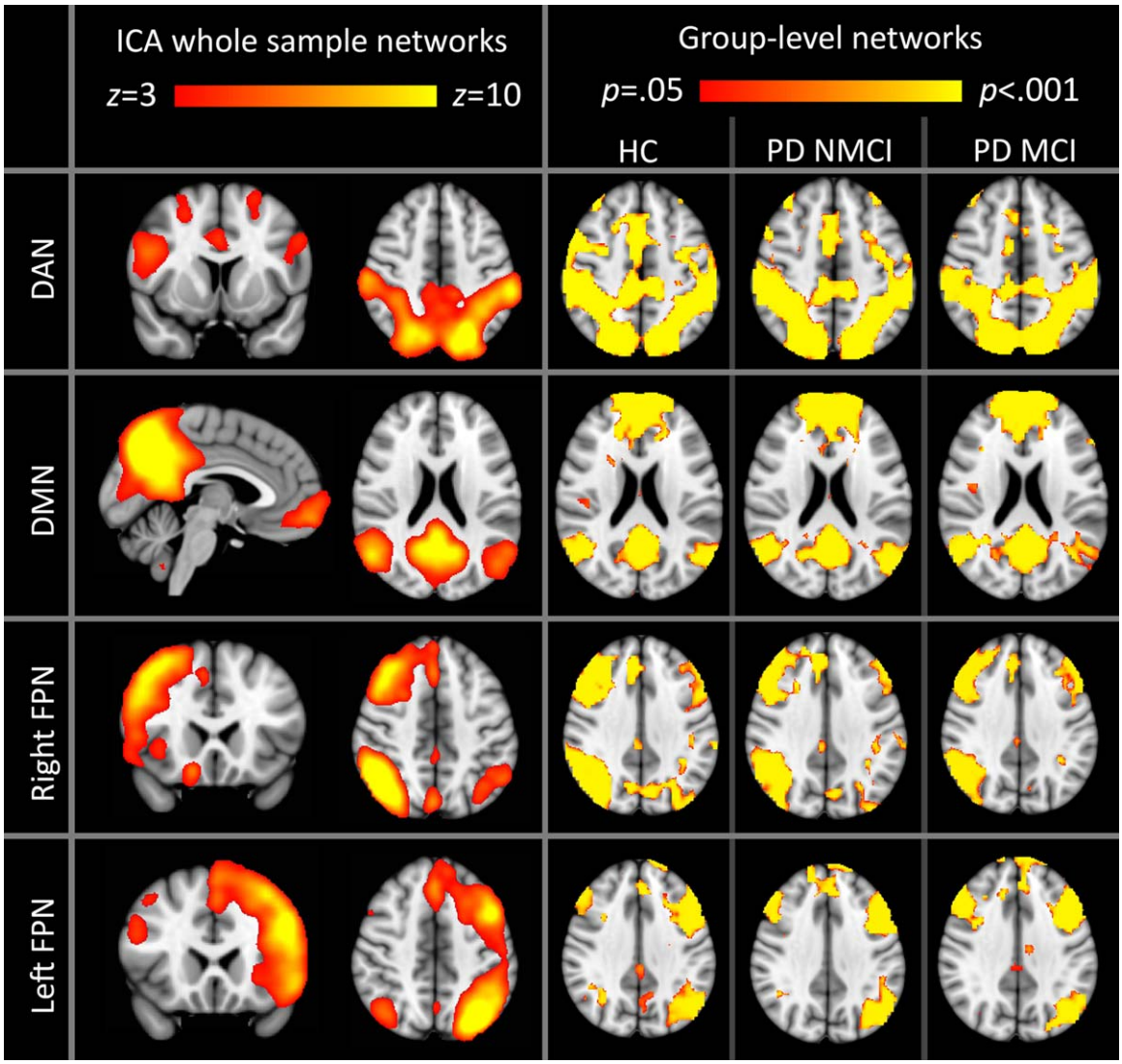

Figure 1.

Resting-state networks of interest. Left-sided images: maps obtained from independent component analyses (ICA) of the whole sample. Right-sided images: group-level maps obtained from dual-regression analyses ($P < 0.05$, FDR corrected). DAN: dorsal attention network; DMN: default-mode network; FPN: frontoparietal network. The right hemisphere is displayed on the left side of axial and coronal views.

internetwork connectivity values (average of the correlation coefficients between nodes according to network affiliation), and (2) between individual intranetwork and internetwork connectivity values (i.e., for connections between every pair of nodes). Permutation testing (10,000 permutations) generating random group affiliation was used to yield a null distribution against which the actual JT test statistics were compared to determine the statistical significance (set at $P < 0.05$) of each interregional connection analysis.

Processing of Structural Images

Structural analyses were done using two different and complementary techniques [Pereira et al., 2012]: VBM to assess GM volume, and cortical thickness (CTh).

VBM: Structural data was analyzed with FSL-VBM [Douaud et al., 2007], a VBM-style analysis. First, structural images were brain-extracted and GM-segmented before being registered to the MNI152 standard space. The resulting images were averaged to create a study-specific

TABLE II. Sociodemographic, clinical, head motion, and white-matter hyperintensity characteristics of participants

		PD		
	HC $n = 36$	Non-MCI $n = 43$	MCI $n = 22$	Test stats/P
Age (yrs.)	63.4 (10.5)	64.0 (9.8)	66.1 (12.2)	0.473/0.624
Sex (female:male)	17:19	20:23	8:14	0.431/0.806 χ
Years of education	10.3 (4.0)	10.8 (5.1)	8.8 (4.0)	2.178/0.119
MMSE	29.70 (.47)	29.35 (0.90)	28.50 (1.22)	**13.285/<0.001**
Hand dominance (*r*:*l*)	34:2	42:1	22:0	2.429/0.657 χ
BDI	5.81 (5.66)	8.9 (6.1)	11.5 (6.6)	**6.357/0.003**
Age at onset (yrs.)	–	57.8 (10.2)	56.8 (13.5)	0.340/0.735†
Disease duration	–	6.1 (4.4)	9.3 (5.5)	**2.523/0.014**†
LEDD	–	646.7 (419.2)	951.9 (498.2)	**2.604/0.011**†
HY (1:2:3)	–	20:21:2	3:15:4	**8.315/0.016** χ
UPDRS-III	–	14.1 (7.5)	18.2 (8.7)	**1.927/0.059**†
Number of outlier timepoints	4.0 (2.6)	3.9 (2.6)	5.3 (3.4)	2.016/0.139
Head rotation (degrees)	0.03 (.01)	0.05 (.04)	0.04 (0.03)	**3.586/0.031**
Head translation (mm)	0.08 (.05)	0.07 (.04)	0.07 (0.05)	0.349/0.706
Normalized WM hyperintensity volume	792.4 (964.0)	792.7 (1278.8)	976.0 (1032.3)	0.230/0.795

Results are presented in means (SD). Statistically significant results ($P < 0.05$) are marked in bold. MMSE: mini-mental state examination. BDI: Beck's Depression Inventory-II scores. Disease duration: duration of motor symptoms, in years. LEDD: Levodopa equivalent daily dose, in mg. HY: Hoehn and Yahr scale. Test stats: *F*-statistics, Pearson's chi-squared (χ) or Student's *t* (†). Post hoc analyses showed significant differences between MCI patients and HC for BDI, between MCI patients and both HC and non-MCI patients for MMSE scores, and between non-MCI patients and healthy controls for head rotation ($P < 0.05$, Bonferroni correction).

template, to which native GM images were nonlinearly re-registered. Second, native GM images were registered to this study-specific template and modulated to correct for local expansion or contraction due to the nonlinear component of the spatial transformation. To perform intergroup connectivity analyses, voxelwise general linear model with nonparametric, permutation testing (5,000 permutations) was applied. FDR was used for multiple comparisons correction ($q < 0.05$).

CTh was estimated using the automated FreeSurfer stream (version 5.1; http://surfer.nmr.harvard.edu). The procedures carried out include the removal of non-brain

TABLE III. Neuropsychological performance results for healthy controls and Parkinson's disease patients according to MCI status

	HC $n = 36$ mean (SD)	PD-NMCI $n = 43$ mean (SD)	PD-MCI $n = 22$ mean (SD)	F/P
VFD	29.61 (2.70)	29.09 (2.34)	26.50 (3.45)	9.550/<0.001
JLO	23.94 (3.99)	23.12 (3.93)	19.50 (5.23)	7.926/0.001
RAVLT total	44.67 (6.05)	44.47 (9.08)	33.55 (7.93)	16.866/0.001
RAVLT retrieval	9.08 (2.10)	8.58 (2.64)	6.05 (2.94)	10.645/<0.001
Digits backwards minus forwards	−1.69 (1.16)	−1.81 (1.03)	−1.23 (1.07)	2.663/0.075
Stroop interference	−2.42 (8.96)	−0.97 (9.92)	−3.31 (5.62)	0.553/0.577
TMT A−B	−50.17 (23.93)	−57.33 (29.58)	−142.35 (104.00)	22.340/<0.001
Phonemic fluency	16.57 (5.03)	16.40 (4.962)	11.82 (5.44)	7.183/0.001
VS/VP *z*-score	−0.012 (0.572)	−0.169 (0.601)	−0.989 (.880)	16.169/<0.001
Memory *z*-score	−0.010 (0.818)	−0.092 (1.028)	−1.365 (1.156)	15.157/<0.001
A/E *z*-score	0.027 (0.537)	−0.022 (0.519)	−0.776 (.996)	12.077/<0.001

Results are presented as means (SD). PD-NMCI: Parkinson's disease patients without MCI; PD-MCI: patients with MCI; VFD: visual form discrimination test; JLO: judgment of line orientation test; RAVLT: Rey's auditory verbal learning test; Digits backwards minus forwards: difference between backward and forward digit spans; TMT A-B: difference between Trail Making Test parts A and B; VS/VP: visuospatial/visuoperceptual; A/E: attention/executive. *Z*-scores for cognitive domains refer to the difference between actual *z*-scores and expected age, sex and education-adjusted *z*-scores, averaged throughout the tests within that domain. For all significant F-test comparisons, post hoc analyses showed that MCI patients' scores were significantly worse than non-MCI patients' and healthy controls', with no significant differences between the latter ($P < 0.05$, post hoc Bonferroni test).

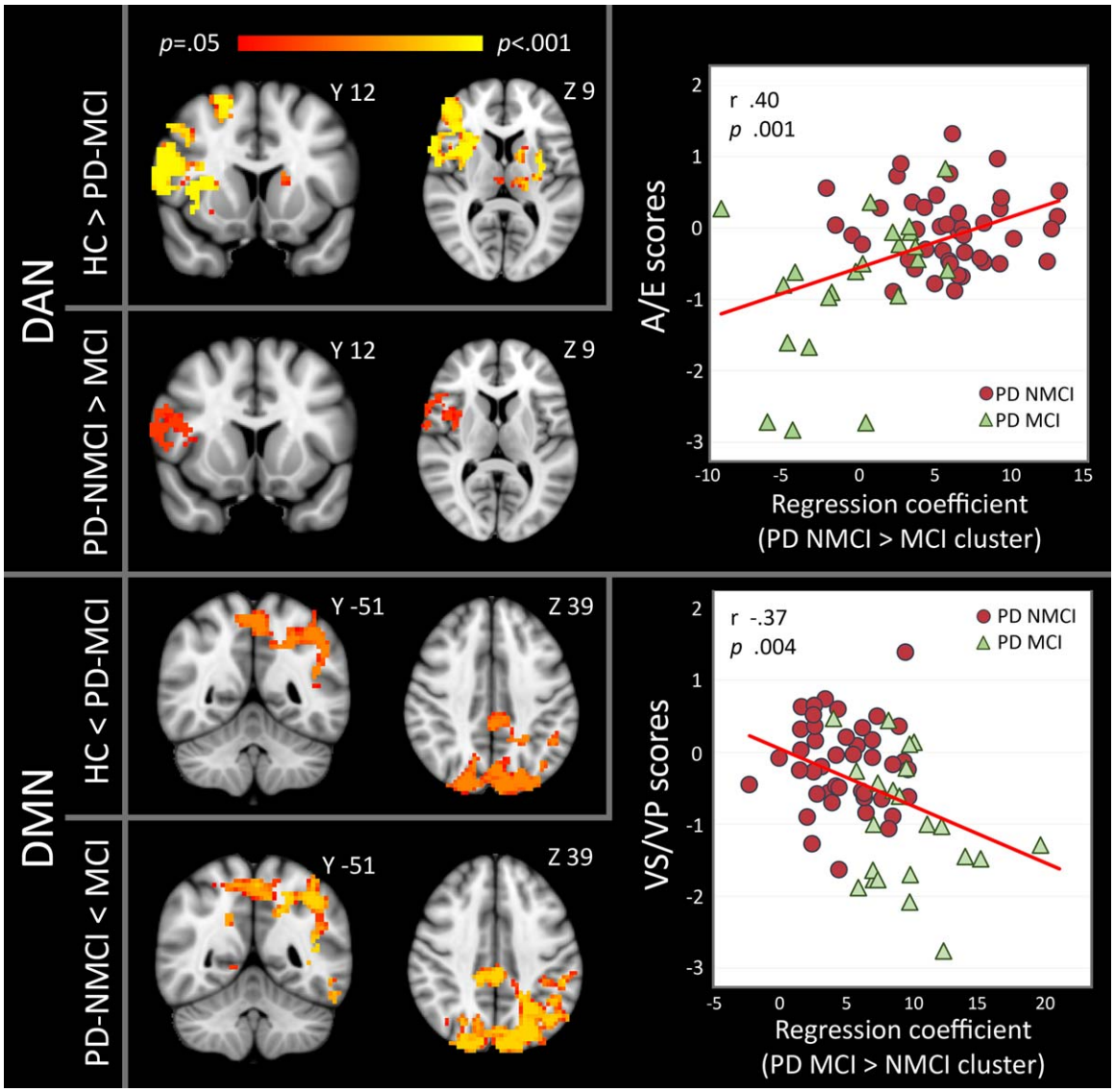

Figure 2.

Data-driven analysis intergroup connectivity comparisons. Left side: clusters of significant ($P < 0.05$, FDR-corrected; 100-voxel threshold) connectivity group differences for PD patients with mild cognitive impairment (PD-MCI) versus HC or patients without mild cognitive impairment (PD-NMCI) for the dorsal attention network (DAN) and the default-mode network (DMN). FDR-corrected *P* values are color-coded according to the bar at the top. MNI *Y* and *Z* coordinates of the slices shown are indicated. Right side: scatterplots showing the correlation between connectivity values (*regression coefficients obtained from the clusters of significant PD-MCI versus PD-NMCI differences) and age-, sex-, and education-corrected z-scores in attention/executive (A/E) and visuospatial/visuoperceptual (VS/VP) functions in the PD patient group. *r*: partial-correlation coefficient. The right hemisphere is displayed on the left side.

data, intensity normalization, tessellation of the GM/WM boundary, automated topology correction [Fischl et al., 2001; Ségonne et al., 2007], and accurate surface deformation to identify tissue borders [Dale et al., 1999; Fischl and Dale, 2000]. Cortical thickness is then calculated as the distance between the white and GM surfaces at each vertex of the reconstructed cortical mantle. Maps were smoothed with an across-surface 15-mm full-width at half maximum circularly symmetric Gaussian kernel.

Intergroup comparisons between groups were performed using a vertex-by-vertex general linear model. All results were corrected for multiple comparisons using

TABLE IV. Clusters of significant intergroup connectivity differences

	Region	MNI152 coordinates of maximum (*x y z*)	Cluster volume (mm^3)	Peak FDR-corrected *P*-value
DAN HC>PD-MCI	Superior frontal gyri, right middle/inferior frontal gyri, right precentral gyrus, right anterior/middle insula	21 36 −15	65,988	0.005
	Right middle temporal gyrus, temporo-occipital junction	60 −57 −6	4,158	0.005
	Left caudate nucleus, left putamen	−12 0 18	3,159	0.005
	Thalami	−6 −15 −3	3,105	0.009
DAN PD-NMCI> PD-MCI	Right inferior frontal gyrus, frontal operculum, anterior/middle insula	57 12 3	7,938	0.038
	Right middle temporal gyrus, temporo-occipital junction	60 −30 −27	3,294	0.038
DMN HC<PD-MCI	Bilateral dorsal precuneus, posterior cingulate gyrus, superior occipito-parietal junctions and superior occipital gyri, left superior parietal lobule	−33 −66 18	42,957	0.034
	Left temporo-occipital junction	−57 −69 −12	4,860	0.034
DMN PD-NMCI <PD-MCI	Bilateral dorsal precuneus, posterior cingulate gyrus, superior occipito-parietal junctions and superior occipital gyri, left superior parietal lobule, left temporo-occipital junction	−57 −21 −27	74,007	0.009

DAN: dorsal attention network; DMN: default mode network; HC: healthy controls; PD-MCI: Parkinson's disease patients with mild cognitive impairment; PD-NMCI: Parkinson's disease patients without mild cognitive impairment.

cluster-wise Monte-Carlo simulation (10,000 iterations). Significance level was set at $P < 0.05$.

To assess the relationship between changes in CTh and cognitive performance, mean thickness values extracted from the clusters of significant group differences were correlated with cognitive function scores (A/E, memory, VS/VP) while controlling for the other two functions and for age (which correlated with CTh values). In addition, to investigate the relationship between structural and functional changes, mean thickness extracted from clusters of significant CTh intergroup differences were correlated with connectivity values extracted from significant functional connectivity differences, controlling for age.

Sociodemographic/Clinical/WM Hyperintensity Data Statistical Analyses

Statistical significance threshold was set at $P < 0.05$. Pearson's chi-squared test was used to compare categorical variables (hand dominance, sex, HY). Student's *t*-test was used to compare head motion, clinical data means between PD patients, and HC. Three-level one-way ANOVAs were used to compare head motion, clinical, WM hyperintensity load, and sociodemographic data between HC and patient subgroups. Significance *P* values were adjusted using post hoc Bonferroni tests.

RESULTS

Table II shows sociodemographic, clinical, head motion, and WM hyperintensity load characteristics for the three groups (HC, non-MCI PD patients [PD-NMCI], MCI PD patients [PD-MCI]). Table III shows neuropsychological assessment results and group comparisons. As expected [Hoops et al., 2009], although subjects' MMSE scores were within the normal range, neuropsychological assessment focusing on specific cognitive functions was able to detect the presence of deficits in a high percentage of patients. Twenty-two patients (33.8%) fulfilled criteria for MCI. VS/VP scores did not correlate significantly with A/E or memory scores, with clinical/demographical variables such as age, education, LEDD, disease duration, or UPDRS-III or BDI scores. A/E scores significantly correlated with memory scores ($r = 0.31$, $P = 0.011$); the latter, in turn, also correlated significantly with LEDD ($r = -0.27$, $P = 0.027$).

Data-Driven Connectivity Analysis

The ICA components corresponding to the ICNs of interest, as well as the areas in all groups that showed to be significantly related to them (one-sample *t*-test, $P < 0.05$,

FDR-corrected) in dual-regression analyses, included, as main regions (see Fig. 1):

DAN: caudal anterior cingulate gyrus, frontal eye fields, dorsolateral prefrontal areas, temporooccipital junctions, and dorsal occipitoparietal regions.

DMN: posterior cingulate gyrus/precuneus, medial prefrontal region, angular gyri, and middle/superior frontal gyri.

Right and left FPN: ipsilateral inferior parietal lobule, lateral prefrontal cortex, insula and opercular region, as well as precuneus.

Intergroup comparisons: No significant differences were observed between HC and the collapsed PD patient group for any of the networks analyzed. Statistically significant group differences were observed when stratifying the PD sample into PD-MCI and PD-NMCI subgroups (see Fig. 2 and Table IV). Compared with HC, the DAN in PD-MCI showed reduced connectivity ($P < 0.05$, FDR-corrected) with widespread, predominantly right sided, frontal/insular areas, as well as with the thalami and left striatum. Connectivity reductions of the DAN in PD-MCI compared with PD-NMCI patients were similar, although less extensive, to those seen between PD-MCI and HC, and involved regions that are part of the DAN itself and of the right FPN (see Fig. 2 and Table IV).

Compared with HC and with PD-NMCI, PD-MCI showed significant connectivity increases ($P < 0.05$, FDR-corrected) between the DMN and posterior cortical regions (see Fig. 2 and Table IV). These regions corresponded to areas of the DAN and the left FPN. No significant connectivity differences were observed between HC and PD-NMCI for any of the ICNs analyzed.

Correlation analyses: Connectivity levels, assessed through the regression coefficients obtained from the clusters of significant differences between PD-MCI and PD-NMCI (DAN and DMN), did not correlate significantly with age, years of education, or BDI/UPDRS-III scores. Connectivity levels in the DAN clusters, conversely, correlated with LEDD ($r = -0.34$, $P = 0.006$).

Partial-correlation analyses evaluating the relationship between connectivity levels in the significant PD-MCI-versus-PD-NMCI comparison clusters and age-, education-, and sex-corrected neuropsychological data revealed:

- significant positive correlation between connectivity in the DAN clusters and A/E scores (partial-correlation coefficient = 0.40, $P = 0.001$).
- significant negative correlation between connectivity in the DMN clusters and VS/VP scores (partial-correlation coefficient= -0.37, $P = 0.004$) and MMSE (partial-correlation coefficient = -0.32, $P = 0.011$) scores.

There were no significant correlations between connectivity values in the clusters of significant intergroup differences and WM hyperintensity load.

Seed-Based A Priori-Defined Connectivity Analysis

Visual inspection confirmed that the a priori masks overlapped with the corresponding regions of the ICNs obtained from ICA. Comparing mean intranetwork and internetwork connectivity values, significant ordered reductions (HC $\geq$ PD-NMCI $\geq$ PD-MCI) were observed in intra-DAN connectivity ($P = 0.036$, 10,000 permutations), and there was suggestive evidence of increases in DAN-DMN internetwork connectivity ($P = 0.067$, 10,000 permutations; see Supporting Information Figure 1). The analysis of individual interregional connections showed that ordered connectivity reductions (HC $\geq$ PD-NMCI $\geq$ PD-MCI) were present both within and between networks (Fig. 3). Intranetwork reductions were found mainly in the DMN and the DAN and were characterized by reductions from positive correlation coefficients in HC to values closer to zero in PD-MCI. Most intra-DMN connectivity reductions involved this ICN's midline nodes and their connections with the left hippocampus, anterior temporal regions and posterior inferior parietal lobules. Intra-DAN reductions were mainly seen between frontal nodes and occipital/parietal nodes. Internetwork connectivity reductions were also observed, mainly affecting connections between the frontal and right insular FPN nodes and occipital/parietal DAN nodes. In HC, these nodes' time series were positively correlated, whereas in PD-MCI they tended to correlate negatively. Connectivity reductions were also seen in a few sparse connections between DAN and DMN nodes.

Connectivity increases (HC $\leq$ PD-NMCI $\leq$ PD-MCI) were also present, involving internetwork connections. Most such increases were found between midline and frontal/temporal DMN nodes and posterior DAN nodes. As expected, in HC these nodes' time series were negatively correlated. In PD-MCI, they tended to be close to zero (see Fig. 3).

See the Supporting Information Table I, for additional information regarding the interregional connections for which significant ordered connectivity effects were observed.

GM Structural Assessment

CTh analyses showed that, compared with HC, PD-MCI subjects had significant cortical thinning in lateral occipital, inferior parietal, and occipito-temporal areas bilaterally, as well as in the left precuneus. PD-NMCI, compared with HC, showed less extensive areas of reduced CTh, also involving lateral occipital regions bilaterally, and in the right middle/inferior temporal gyrus (see Fig. 4 and the Supporting Information Table II). No significant differences were observed between PD-MCI and PD-NMCI.

Partial-correlation analyses evaluating the relationship between mean cortical thickness in the significant HC-versus-PD-NMCI and HC-versus-PD-MCI comparison clusters and neuropsychological and connectivity values revealed (see Supporting Information Figure 2):

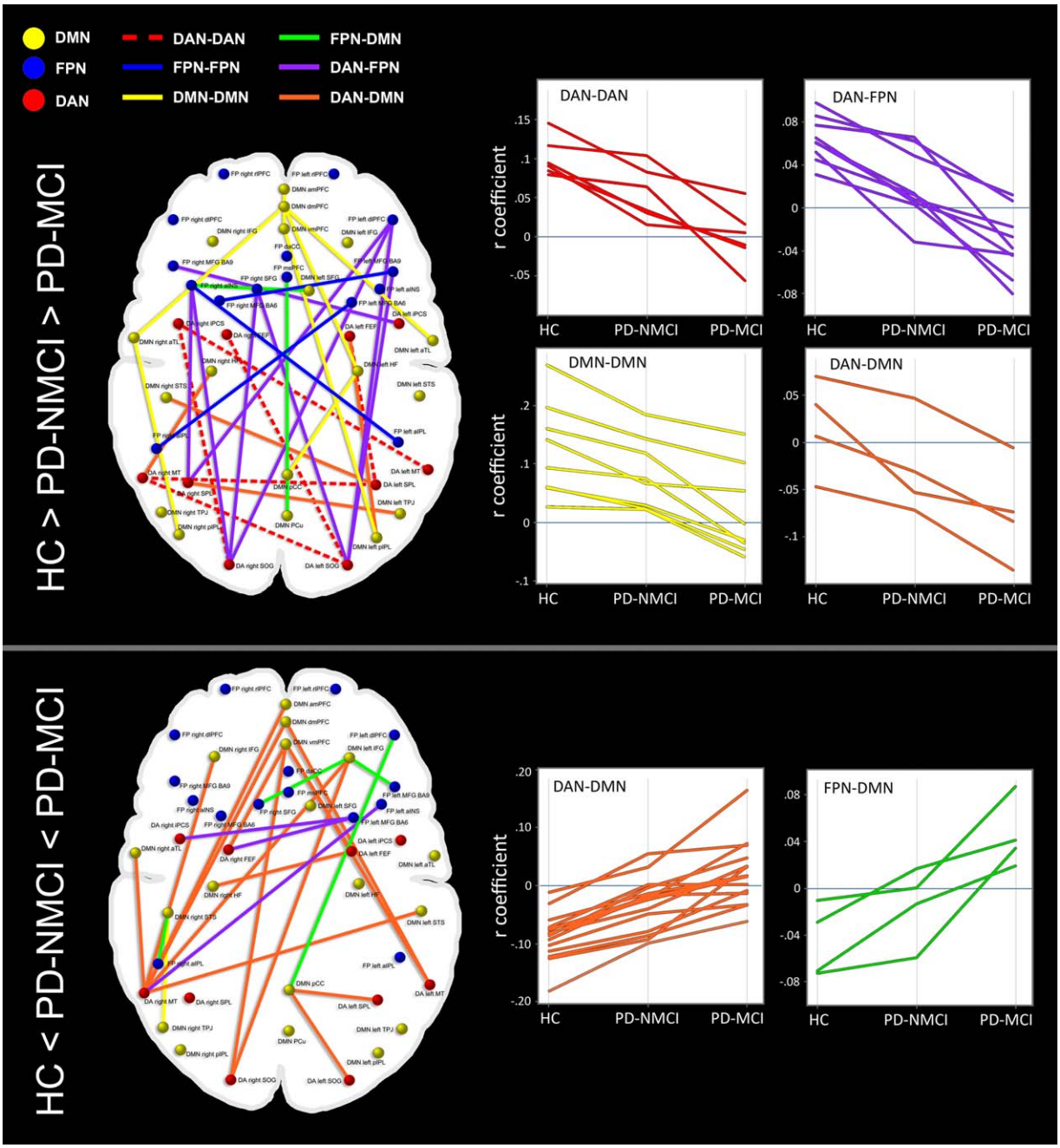

Figure 3.

Seed-based connectivity analysis results. Left side: schematic representation of the interregional connections where significant ($P < 0.05$) ordered connectivity changes were observed. Network affiliation of the nodes shown as well as of the internodal connections is indicated in the legend above. Abbreviations refer to those described in Table I. Right side: plots showing *r* coefficient levels according to group for the connections where significant effects were found, according to the network affiliation of the involved nodes. Only intranetwork or internetwork changes comprising more than three connections are plotted. DAN: dorsal attention network; DMN: default-mode network; FPN: frontoparietal network; HC: healthy controls; PD-NMCI: Parkinson's disease patients without mild cognitive impairment; PD-MCI: Parkinson's disease patients with mild cognitive impairment.

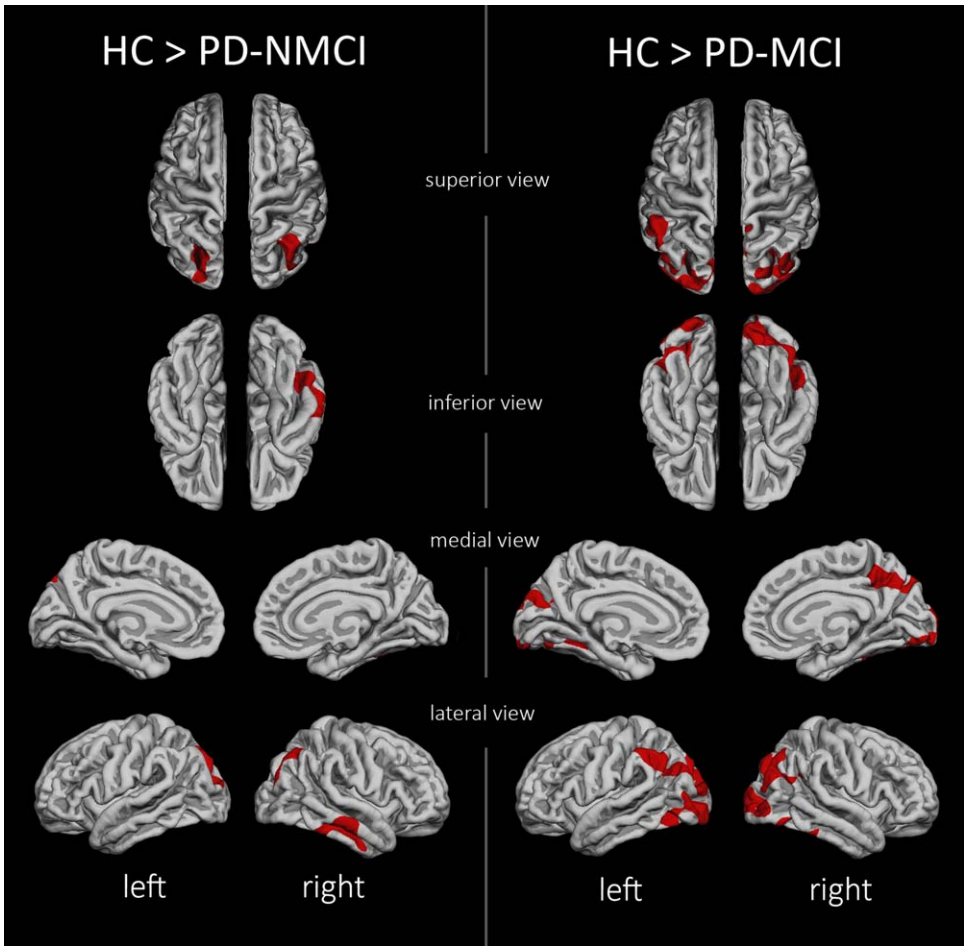

Figure 4.

Vertexwise comparison of cortical thickness between HC, Parkinson's disease patients without mild cognitive impairment (PD-NMCI), and Parkinson's disease patient with mild cognitive impairment (PD-MCI). Red clusters indicate areas of significantly reduced cortical thickness in PD-NMCI compared with HC (left) and in PD-MCI compared with HC (right; $P < 0.05$). [Color figure can be viewed in the online issue, which is available at wileyonlinelibrary.com.]

- positive correlation between CTh in the left-sided lateral occipital/temporo-occipital HC-versus-PD-MCI cluster and VS/VP scores (partial-correlation coefficient = 0.26, $P = 0.042$).
- negative correlation between CTh in the left-sided lateral occipital/temporo-occipital HC-versus-PD-MCI cluster and connectivity levels in the clusters of increased connectivity between the DMN and occipito-parietal regions in PD-MCI compared with PD-NMCI (partial-correlation coefficient $= -0.26$, $P = 0.038$) and in PD-MCI compared with controls (partial-correlation coefficient $= -0.28$, $P = 0.025$).

No significant intergroup differences or correlations with neuropsychological scores were found for mean CTh. In accordance with previous studies that described a higher sensitivity of CTh in the detection of PD-related structural atrophy, no significant intergroup GM volume differences were observed with VBM [Pereira et al., 2012].

DISCUSSION

In this study, we investigated the resting-state functional connectivity of brain ICNs in PD patients according to the presence or absence of MCI using two complementary techniques. As main findings, we observed that PD patients with MCI had a reduction in connectivity between right frontoinsular regions and the DAN, associated with A/E performance; and an increased connectivity between posterior cortical regions—where there was also evidence of structural degeneration—and the DMN, associated with VS/VP scores.

Previous studies have described an association between changes in DMN connectivity and neuropsychological performance in distinct neurological and psychiatric diseases (see [Mevel et al., 2011] and [Whitfield-Gabrieli and Ford, 2012]), but little is known about how changes in internetwork connectivity relate to cognitive decline. Previous fMRI studies show that, during externally-directed cognitive tasks, DAN activity increases whereas DMN activity is reduced; during "rest" or internally-directed/self-referential thoughts, the opposite is observed [Kelly et al., 2008]. The FPN, functionally and anatomically interposed between the main DMN and DAN nodes, has been postulated to flexibly connect to one network or the other depending on attentional task demands, mediating the transition between them [Spreng et al., 2013; Vincent et al., 2008]. This transition appears to be relevant for cognitive task performance [Kelly et al., 2008]. In this work, PD-MCI subjects displayed reduced connectivity between the DAN and the right anterior insula and adjacent frontal areas, which are regions of the DAN itself and of the right FPN—networks that are considered to play a role in attentional processes [Hellyer et al., 2014]. Furthermore, the relevance of the frontoinsular cortex in cognition has recently been demonstrated (see [Christopher et al., 2014a]). Importantly, this region has been shown to exert a critical and causal role in switching between DAN and DMN across tasks of different modalities, as well as in the resting state [Sridharan et al., 2008]. In PD patients with visual hallucinations, insular GM volume was seen to correlate with DAN activation during a visual task [Shine et al., 2014]. We have found that reduced connectivity—without detectable associated structural atrophy—between this area and the DAN in PD patients was associated with worse performance in A/E functions, suggesting that functional right frontoinsular cortical changes are involved in this type of deficit in PD. It could be speculated that this association is related to impaired network-switching mechanisms, a hypothesis that could be assessed by future, task-based fMRI studies.

In healthy persons, dopamine synthesis capacity has been shown to correlate with reduced DAN-FPN and increased FPN-DMN coupling, during the resting state [Dang et al., 2012]. Importantly, a recent study found that PD-MCI patients have reduced insular dopaminergic D2 receptors, and that this loss is associated with worse performance in executive functions [Christopher et al., 2014b]. Taken together with our findings, these data indicate that A/E deficits in PD—considered to be related to frontostriatal dopaminergic imbalances (see [Cools and D'Esposito, 2011])—may be mediated by dopaminergic effects on DAN connectivity.

In this study, PD-MCI subjects displayed increased connectivity between the DMN and occipito-parietal lateral and medial cortical regions that are components of the left FPN and the DAN. Seed-based analyses also revealed an increased connectivity between DMN and posterior DAN nodes in PD-MCI, characterized by the loss of the negative correlation normally observed between these regions. Despite variable findings regarding the DMN in PD, the most frequently described connectivity changes involve abnormal patterns of activation and deactivation of the precuneus/PCC during rest and cognitive tasks [Eimeren and Monchi, 2009]. In this study, connectivity increments between the DMN and occipito-parietal cortical areas were seen to be associated with worse VS/VP performance. Seed-based analyses revealed reduced within-DMN connectivity, a finding in line with a recent resting-state fMRI study that evaluated cognitively unimpaired PD patients [Tessitore et al., 2012]. As in this study, connectivity changes affecting posterior cortical regions correlated with performance in VS/VP tests. Interestingly, we also found cortical thinning in occipito-parietal regions in the PD patient group, more markedly in the PD-MCI subgroup, which also showed a relationship with VS/VP performance. These findings are in line with and complement previous structural neuroimaging studies addressing the neuroanatomical bases of VS/VP deficits in PD [Pereira et al., 2009]. Furthermore, previous evidence suggests that task-positive FPN and the DMN competitively connect with visual areas during visual tasks, and that the degree of decoupling of the DMN with these structures predicts task performance [Chadick and Gazzaley, 2011]. Our findings suggest that changes in connectivity between the DMN and posterior cortical areas belonging to the DAN and the FPN may be part of the substrates of VS/VP deficits in PD through a disruption of these dynamic coupling mechanisms.

Longitudinal studies have shown that, unlike dopamine-related deficits, impairments with posterior cortical bases are predictors of future dementia in PD [Williams-Gray et al., 2007; Williams-Gray et al., 2009]. Data from a longitudinal PET study found that reduced glucose metabolism in occipital and posterior cingulate regions heralded future conversion to dementia [Bohnen et al., 2011], emphasizing the importance of posterior cortical changes as predictors of dementia in PD. We hypothesize that the connectivity increases observed, as well as the structural atrophy seen to be associated with it, are related to the cortical dysfunctions that lead to progressive cognitive decline and, ultimately, dementia. As with current evidence this association is speculative, however, it remains to be studied whether these occipito-parieto-temporal connectivity and structural changes are related to the cortical pathology that appears to be critical for the development of dementia in PD, such as synucleinopathy or Alzheimer's-type pathology [Compta et al., 2011].

The finding of increased functional connectivity associated with worse cognitive status merits further discussion. Increased functional connectivity is a frequent finding in neurological diseases of different nature [Hillary et al., in press; Pievani et al., 2011]. In this study, however, connectivity increments were primarily observed in internetwork connections. Specifically, seed-based analyses showed that these connectivity increases predominantly involved the loss of the normal pattern of anti-correlation between

DMN nodes and parietal, occipital and temporal DAN nodes in PD-MCI; the latter nodes were also seen to be less connected to other DAN and FPN nodes. Instead of an actual direct increase in connectivity, at least part of the observed effect might be mediated by the reduced connectivity of DAN nodes with their parent network; being less connected to other DAN regions, these nodes may also lose the expected negative correlation this network displays with the DMN.

One possible limitation of our study is that, despite the rigorous head motion exclusion criteria and preprocessing steps aimed at minimizing the effect of motion artifacts, we cannot guarantee that our results were not influenced to some degree by them. Nonetheless, the identified connectivity effects were more pronounced in PD-MCI, which had less head motion than the PD-NMCI group. These observations suggest that our results have actual biological origins. Furthermore, patients in our study were assessed in the *on* state, that is, under the effect of dopaminergic medication, which influences ICN connectivity [Cole et al., 2013; Dang et al., 2012]. Although this may limit the assessment of PD-related effects on the studied ICNs, our goal was to evaluate the substrate of the cognitive deficits as they occur in patients' daily lives—under the influence of their usual medication. Furthermore, our results were maintained when adding LEDD as a covariate, suggesting that the connectivity changes observed go beyond the effects of dopaminergic medication. As this may not entirely control for the acute and chronic effects of dopaminergic therapy, however, future studies including both *on* and *off*-state assessments, as well as drug-naïve subjects, could provide useful additional information.

This study shows that cognitive decline in PD is associated with different patterns of connectivity changes affecting large-scale brain ICNs. These findings suggest that network changes, mainly characterized by the loss of intra-network connectivity and an increase in the connectivity between networks that normally display anti-correlated activities, are part of the neural substrate underlying cognitive deficits in PD. Moreover, our results give support to the hypothesis that the brain networks studied play a role in the neural processing of distinct neuropsychological functions. Future, longitudinal studies may help establish a potential role for ICN connectivity measures as predictors of cognitive decline in PD.

ACKNOWLEDGMENT

The authors M.J.M., R.S., F.V., and Y.C. report no disclosures.

REFERENCES

Aarsland D, Kurz MW (2010): The epidemiology of dementia associated with Parkinson disease. J Neurol Sci 289:18–22.

Aarsland D, Brønnick K, Larsen JP, Tysnes OB, Alves G (2009): Cognitive impairment in incident, untreated Parkinson disease: The Norwegian ParkWest study. Neurology 72:1121–1126.

Agosta F, Pievani M, Geroldi C, Copetti M, Frisoni GB, Filippi M (2012): Resting state fMRI in Alzheimer's disease: Beyond the default mode network. Neurobiol Aging 33:1564–1578.

Baggio H-C, Sala-Llonch R, Segura B, Marti M-J, Valldeoriola F, Compta Y, Tolosa E, Junqué C (2014): Functional brain networks and cognitive deficits in Parkinson's disease. Hum Brain Mapp 35:4620–4634.

Beckmann CF, Smith SM (2004): Probabilistic independent component analysis for functional magnetic resonance imaging. IEEE Trans Med Imaging 23:137–152.

Bewick V, Cheek L, Ball J (2004): Statistics review 10: Further nonparametric methods. Crit Care 8:196–199.

Bohnen NI, Koeppe RA, Minoshima S, Giordani B, Albin RL, Frey KA, Kuhl DE (2011): Cerebral glucose metabolic features of Parkinson disease and incident dementia: Longitudinal study. J Nucl Med 52:848–855.

Brier MR, Thomas JB, Snyder AZ, Benzinger TL, Zhang D, Raichle ME, Holtzman DM, Morris JC, Ances BM (2012): Loss of intranetwork and internetwork resting state functional connections with Alzheimer's disease progression. J Neurosci 32: 8890–8889.

Chadick JZ, Gazzaley A (2011): Differential coupling of visual cortex with default or frontal-parietal network based on goals. Nat Neurosci 14:830–832.

Christopher L, Koshimori Y, Lang AE, Criaud M, Strafella AP (2014a): Uncovering the role of the insula in non-motor symptoms of Parkinson's disease. Brain 137:2143–2154.

Christopher L, Marras C, Duff-Canning S, Koshimori Y, Chen R, Boileau I, Segura B, Monchi O, Lang AE, Rusjan P, Houle S, Strafella AP (2014b): Combined insular and striatal dopamine dysfunction are associated with executive deficits in Parkinson's disease with mild cognitive impairment. Brain 137:565–575.

Cole DM, Beckmann CF, Oei NYL, Both S, van Gerven JMA, Rombouts SA RB (2013): Differential and distributed effects of dopamine neuromodulations on resting-state network connectivity. Neuroimage 78:59–67.

Compta Y, Parkkinen L, O'Sullivan SS, Vandrovcova J, Holton JL, Collins C, Lashley T, Kallis C, Williams DR, de Silva R, Lees AJ, Revesz T (2011): Lewy- and Alzheimer-type pathologies in Parkinson's disease dementia: Which is more important? Brain 134:1493–1505.

Cools R, D'Esposito M (2011): Inverted-U-shaped dopamine actions on human working memory and cognitive control. Biol Psychiatry 69:e113–e125.

Dale AM, Fischl B, Sereno MI (1999): Cortical surface-based analysis. I. Segmentation and surface reconstruction. Neuroimage 9: 179–194.

Dang LC, O'Neil JP, Jagust WJ (2012): Dopamine supports coupling of attention-related networks. J Neurosci 32:9582–9587.

Douaud G, Smith S, Jenkinson M, Behrens T, Johansen-Berg H, Vickers J, James S, Voets N, Watkins K, Matthews PM, James A (2007): Anatomically related grey and white matter abnormalities in adolescent-onset schizophrenia. Brain 130:2375–2386.

Eimeren MT van, Monchi O (2009): Dysfunction of the Default Mode Network in Parkinson Disease. Arch Neurol 66:877–883.

Elgh E, Domellöf M, Linder J, Edström M, Stenlund H, Forsgren L (2009): Cognitive function in early Parkinson's disease: A population-based study. Eur J Neurol 16:1278–1284.

Emre M, Aarsland D, Brown R, Burn DJ, Duyckaerts C, Mizuno Y, Broe GA, Cummings J, Dickson DW, Gauthier S, Goldman

J, Goetz C, Korczyn A, Lees A, Levy R, Litvan I, McKeith I, Olanow W, Poewe W, Quinn N, Sampaio C, Tolosa E, Dubois B (2007): Clinical diagnostic criteria for dementia associated with Parkinson's disease. Mov Disord 22:1689–1707; quiz 1837.

Filippini N, MacIntosh BJ, Hough MG, Goodwin GM, Frisoni GB, Smith SM, Matthews PM, Beckmann CF, Mackay CE (2009): Distinct patterns of brain activity in young carriers of the APOE-epsilon4 allele. Proc Natl Acad Sci USA 106:7209–7214.

Fischl B, Dale AM (2000): Measuring the thickness of the human cerebral cortex from magnetic resonance images. Proc Natl Acad Sci USA 97:11050–11055.

Fischl B, Liu A, Dale AM (2001): Automated manifold surgery: Constructing geometrically accurate and topologically correct models of the human cerebral cortex. IEEE Trans Med Imaging 20:70–80.

Fox MD, Corbetta M, Snyder AZ, Vincent JL, Raichle ME (2006): Spontaneous neuronal activity distinguishes human dorsal and ventral attention systems. Proc Natl Acad Sci USA 103:10046–10051.

Hellyer PJ, Shanahan M, Scott G, Wise RJS, Sharp DJ, Leech R (2014): The control of global brain dynamics: Opposing actions of frontoparietal control and default mode networks on attention. J Neurosci 34:451–461.

Hillary FG, Roman CA, Venkatesan U, Rajtmajer SM, Bajo R, Castellanos ND: Hyperconnectivity is a Fundamental Response to Neurological Disruption (in press).

Hoops S, Nazem S, Siderowf AD, Duda JE, Xie SX, Stern MB, Weintraub D (2009): Validity of the MoCA and MMSE in the detection of MCI and dementia in Parkinson disease. Neurology 73:1738–1745.

Ithapu V, Singh V, Lindner C, Austin BP, Hinrichs C, Carlsson CM, Bendlin BB, Johnson SC (2014): Extracting and summarizing white matter hyperintensities using supervised segmentation methods in Alzheimer's disease risk and aging studies. Hum Brain Mapp 4235:4219–4235.

Kelly AMC, Uddin LQ, Biswal BB, Castellanos FX, Milham MP (2008): Competition between functional brain networks mediates behavioral variability. Neuroimage 39:527–537.

Krajcovicova L, Mikl M, Marecek R, Rektorova I (2012): The default mode network integrity in patients with Parkinson's disease is levodopa equivalent dose-dependent. J Neural Transm 119:443–454.

Liu Y, Liang M, Zhou Y, He Y, Hao Y, Song M, Yu C, Liu H, Liu Z, Jiang T (2008): Disrupted small-world networks in schizophrenia. Brain 131:945–961.

Mevel K, Chételat G, Eustache F, Desgranges B (2011): The default mode network in healthy aging and Alzheimer's disease. Int J Alzheimers Dis 2011:535816.

Muslimovic D, Post B, Speelman JD, Schmand B (2005): Cognitive profile of patients with newly diagnosed Parkinson disease. Neurology 65:1239–1245.

Pereira JB, Junqué C, MartÚ M-J, Ramirez-Ruiz B, Bargalló N, Tolosa E (2009): Neuroanatomical substrate of visuospatial and visuoperceptual impairment in Parkinson's disease. Mov Disord 24:1193–1199.

Pereira JB, Ibarretxe-Bilbao N, Marti M-J, Compta Y, Junqué C, Bargallo N, Tolosa E (2012): Assessment of cortical degeneration in patients with Parkinson's disease by voxel-based morphometry, cortical folding, and cortical thickness. Hum Brain Mapp 33:2521–2534.

Pievani M, de Haan W, Wu T, Seeley WW, Frisoni GB (2011): Functional network disruption in the degenerative dementias. Lancet Neurol 10:829–843.

Power JD, Barnes KA, Snyder AZ, Schlaggar BL, Petersen SE (2012): Spurious but systematic correlations in functional connectivity MRI networks arise from subject motion. Neuroimage 59:2142–2154.

Raichle ME (2011): The restless brain. Brain Connect 1:3–12.

Rektorova I, Krajcovicova L, Marecek R, Mikl M (2012): Default mode network and extrastriate visual resting state network in patients with Parkinson's disease dementia. Neurodegener Dis 10:232–237.

Sala-Llonch R, Arenaza-Urquijo EM, Valls-Pedret C, Vidal-Piñeiro D, Bargalló N, Junqué C, Bartrés-Faz D (2012): Dynamic functional reorganizations and relationship with working memory performance in healthy aging. Front Hum Neurosci 6:152.

Seeley WW, Menon V, Schatzberg AF, Keller J, Glover GH, Kenna H, Reiss AL, Greicius MD (2007): Dissociable intrinsic connectivity networks for salience processing and executive control. J Neurosci 27:2349–2356.

Ségonne F, Pacheco J, Fischl B (2007): Geometrically accurate topology-correction of cortical surfaces using nonseparating loops. IEEE Trans Med Imaging 26:518–529.

Shine JM, Halliday GM, Gilat M, Matar E, Bolitho SJ, Carlos M, Naismith SL, Lewis SJG (2014): The role of dysfunctional attentional control networks in visual misperceptions in Parkinson's disease. Hum Brain Mapp 35:2206–2219.

Smith SM, Fox PT, Miller KL, Glahn DC, Fox PM, Mackay CE, Filippini N, Watkins KE, Toro R, Laird AR, Beckmann CF (2009): Correspondence of the brain's functional architecture during activation and rest. Proc Natl Acad Sci USA 106:13040–13045.

Spreng RN, Stevens WD, Chamberlain JP, Gilmore AW, Schacter DL (2010): Default network activity, coupled with the frontoparietal control network, supports goal-directed cognition. Neuroimage 53:303–317.

Spreng RN, Sepulcre J, Turner GR, Stevens WD, Schacter DL (2013): Intrinsic architecture underlying the relations among the default, dorsal attention, and frontoparietal control networks of the human brain. J Cogn Neurosci 25:74–86.

Sridharan D, Levitin DJ, Menon V (2008): A critical role for the right fronto-insular cortex in switching between central-executive and default-mode networks. Proc Natl Acad Sci USA 105: 12569–12574.

Tessitore A, Esposito F, Vitale C, Santangelo G, Amboni M, Russo A, Corbo D, Cirillo G, Barone P, Tedeschi G (2012): Default-mode network connectivity in cognitively unimpaired patients with Parkinson disease. Neurology 79:2226–2232.

Tomlinson CL, Stowe R, Patel S, Rick C, Gray R, Clarke CE (2010): Systematic review of levodopa dose equivalency reporting in Parkinson's disease. Mov Disord 25:2649–2653.

Vincent JL, Kahn I, Snyder AZ, Raichle ME, Buckner RL (2008): Evidence for a frontoparietal control system revealed by intrinsic functional connectivity. J Neurophysiol 100:3328–3342.

Whitfield-Gabrieli S, Ford JM (2012): Default mode network activity and connectivity in psychopathology. Annu Rev Clin Psychol 8:49–76.

Williams-Gray CH, Foltynie T, Brayne CEG, Robbins TW, Barker RA (2007): Evolution of cognitive dysfunction in an incident Parkinson's disease cohort. Brain 130:1787–1798.

Williams-Gray CH, Evans JR, Goris A, Foltynie T, Ban M, Robbins TW, Brayne C, Kolachana BS, Weinberger DR, Sawcer SJ, Barker RA (2009): The distinct cognitive syndromes of Parkinson's disease: 5 year follow-up of the CamPaIGN cohort. Brain 132:2958–2969.